JOURNAL OF CATALYSIS **169,** 423–437 (1997)
ARTICLE NO. CA971718

Gas-Uptake, Methanation, and Microcalorimetric Measurements on the Coadsorption of CO and H_2 over Polycrystalline Ru and a Ru/TiO_2 Catalyst

N. M. Gupta, V. P. Londhe, and V. S. Kamble

Chemistry Division, Bhabha Atomic Research Centre, Trombay, Mumbai 400085, India

Received September 9, 1996; revised April 7, 1997; accepted April 9, 1997

The adsorption, methanation, and heat evolved over a Ru/TiO_2 catalyst were found to be quite different than that over a polycrystalline Ru sample, when exposed to $CO + H_2$ (1 : 4) pulses at different temperatures in the range 300–470 K. The coadsorbed H_2 is found to have a large promotional effect on the CO uptake by the Ru/TiO_2 catalyst, the extent of which depended on the catalyst temperature and the surface coverage. No such effect was observed in the case of Ru metal. Thus, while using Ru/TiO_2 the ratio $H_{2(ad)}/CO_{(ad)}$ increased progressively from 0.7 to 4 with the rise in catalyst temperature from 300 to 470 K, it was almost constant at $\sim 5 \pm 0.5$ in the case of ruthenium metal. The exposure of Ru metal to $CO + H_2$ (1 : 4) pulses gave rise to a differential heat of adsorption (q_d) $\sim$ 50 kJ mol^{-1} at all the reaction temperatures under study, which corresponded to adsorption of CO and H_2 molecules at distinct metal sites and in 1 : 1 stoichiometry. In the presence of excess H_2, a q_d value of $\sim$180–190 kJ mol^{-1} was observed at the reaction temperatures above 425 K, suggesting the simultaneous hydrogenation of C_s species formed during CO dissociation. Contrary to this, a $q_d \sim 115$ kJ mol^{-1} was observed for the $CO + H_2$ (1 : 4) pulse injection over Ru/TiO_2 at 300 K, the value reducing to $\sim$70 kJ mol^{-1} at higher reaction temperatures. Furthermore, a lower q_d value ($\sim$50 kJ mol^{-1}) was observed during CO adsorption over Ru/TiO_2 at 300 K in the presence of excess H_2, which increased to $\sim$250 kJ mol^{-1} for the sample temperatures of 420 and 470 K. These data are consistent with the FTIR spectroscopy results on $CO + H_2$ adsorption over Ru/TiO_2 catalyst, showing the formation of $Ru(CO)_n$, $RuH(CO)_n$, and $RuH(CO)_{n-1}$ type surface complexes ($n = 2$ or 3) in addition to the linear or the bridge-bonded CO molecules held at the large metal cluster sites (Ru_xCO). The relative intensity of IR bands responsible to these species depended on the catalyst temperature, the Ru_xCO species growing progressively with the temperature rise. In the case of Ru metal, the formation of only linearly held surface species is envisaged. Arguments are presented to suggest that the CO molecules adsorbed in the multicarbonyl form require lesser energy to dissociate and are therefore responsible to the observed low temperature (<450 K) methanation activity of Ru/TiO_2. On the other hand, the activity at the higher reaction temperatures, both for the Ru metal and for the Ru/TiO_2 catalyst, arises due to dissociation of the linearly or bridge-bonded CO molecules. The Ru–C_n and Ru–C species formed during dissociation of multicarbonyls and linearly bonded CO, respectively, are envisaged to have different rates of graphitization, the former species causing a rapid catalyst deactivation at the lower temperatures.

INTRODUCTION

In the earlier part of this study (1) we reported on adsorption and microcalorimetric measurements on the polycrystalline Ru metal and a Ru(4.5 wt%)/TiO_2 catalyst exposed to successive pulses of CO and H_2 at different temperatures in the range 300–470 K. The differential heats (q_d) at the initial stages of CO and H_2 adsorption at room temperature over ruthenium metal were found to be 120 and 65 kJ mol^{-1}, respectively. The corresponding values in the case of Ru/TiO_2 were 130 and 57 kJ mol^{-1}. The two catalysts, however, showed entirely different adsorption behavior at the higher sample temperatures and for the increasing surface coverages, as is described in (1) in detail. In continuation, the present paper deals with the results of similar investigations on CO and H_2 coadsorption. The objective of this study was to delineate the reaction routes involved in the CO methanation reaction over the bulk and the supported forms of Ru metal. FTIR spectroscopy study on $CO + H_2$ adsorption over Ru/TiO_2 catalyst was carried out in order to identify the surface transient species associated with the microcalorimetry and the gas chromatography data.

EXPERIMENTAL

Catalytic Activity

The preparation method and the characteristics of a Ru(4.5 wt%)/TiO_2 catalyst and the polycrystalline ruthenium metal powder used in this study are given in Ref. (1). A 40–80 mesh fraction of both of the catalysts was normally used for these measurements. As mentioned in (1), even though the BET surface areas of two samples were quite different, their metal surface areas were comparable.

The catalyst activity was evaluated at atmospheric pressure and in the temperature range 300–700 K, using

0021-9517/97 $25.00

0.5-g lot of a sample loaded in a conventional quartz microreactor. $CO + H_2$ (1 : 4) gas mixture was passed at a flow rate of 0.5 lph and the effluents sampled at regular intervals were analyzed with the help of a gas chromatograph equipped with a thermal conductivity detector and a Porapak-Q column, both maintained at 300 K. The CO methanation reaction was also studied in the two other modes, in order to get the comparative activity data unaffected by C-poisoning and under different H_2 concentration conditions. For this purpose, 100-μl (4.1 μmol) pulses of CO were dosed into H_2 carrier gas flowing (30 ml min^{-1}) over catalyst bed at different temperatures. alternatively, 100-μl pulses of $CO + H_2$ (1 : 4) were dosed into He carrier gas (30 ml min^{-1}) passing over catalyst bed. The reaction products were analyzed by a GC connected on line.

Microcalorimetry

A microcalorimeter (C-80 Cetaram, France) equipped with gas circulation cells and connected at the outlet to a GC was employed to measure the enthalpy changes during the $CO + H_2$ reaction under different test conditions. The details of this equipment and the measurement procedures are described in Ref. (1). A fresh lot of 100 mg catalyst (40–80 mesh fraction) was used for each study. After activation under H_2 flow (20 ml min^{-1}, 475 K, 2 h), followed by evacuation (475 K, 1 h) and heating in He (20 ml min^{-1}, 475 K, 1 h), the catalyst was maintained under helium flow and was then dosed with several successive 4.1-μmol pulses of $CO + H_2$ (1 : 4) at a desired temperature. The interval between the two pulse injections was about 15 min. The heat evolved and the reaction products, if any, were analyzed simultaneously.

FTIR Spectroscopy

A Mattson Cygnus-100 FTIR spectrometer equipped with a DTGS detector was used in this study. For each spectrum, 300 scans were normally recorded in the transmittance mode and at a 4 cm^{-1} resolution. A stainless-steel cell equipped with water-cooled CaF_2 windows was used to record the IR spectrum of a 25-mm diameter self-supporting wafer (~80 mg) of Ru/TiO_2 after exposure to $CO + H_2$ (1 : 4) at the different temperatures in the range 300–475 K. The details of the IR cell and the adopted procedure are given elsewhere (2–4). Before recording a spectrum, the sample was activated (570 K, 2 h) under H_2 flow followed by evacuation at 570 K. A deconvolution program in the instrument software was used to discern the overlapping bands (4). The deconvolution parameters chosen for this purpose were full width at half maximum (w) = 30, enhancement factor (k) = 1.2, fraction Lorentzian (f) = 0.3, and the apodization or smoothing function (a) = 3 (Bassel).

RESULTS

Catalyst Activity

Ru/TiO_2. Curve a in Fig. 1 presents the initial catalyst activity of Ru/TiO_2 catalyst when $CO + H_2$ (1 : 4) reacted in the flow mode at different temperatures. The catalyst showed poor activity at reaction temperatures less than 500 K. Also, the catalyst was found to deactivate rapidly after about 15–20 min at these temperatures. However, almost 100% conversion of CO to CH_4 occurred at the temperatures of 575 K and above corresponding to a turnover frequency of around 90×10^{-3} CH_4 molecules per metal site per second, which is comparable with the values reported by Vannice and Garten (6) for titania-supported ruthenium catalysts. Unlike at lower reaction temperatures, the catalyst activity was found to sustain for several hours of study at reaction temperatures above 570 K. The time-dependent variation of the catalytic activity at different reaction temperatures in shown in the inset of Fig. 1. The low-temperature methane yields were, however, higher when the reaction was carried out in the pulse mode and in the presence of excess H_2. Thus, the curve b in Fig. 1 shows methane yield when 4.1-μmol pulses of $CO + H_2$ (1 : 4) were dosed at regular intervals while maintaining the catalyst under He flow (30 ml min^{-1}). On the other hand, curve c shows these data for the CO pulse exposures made in the presence of H_2 carries gas (30 ml min^{-1}). Data in Fig. 1c show that up to 50% of the dosed CO was methanated at a reaction temperature as low as 375 K, for very high H_2/CO stoichiometry in the reacting stream.

In addition to methane, small amount of ethane was also formed only under the reaction conditions of curve c. The ethane formation commenced at 370 K and reached a saturation value (~11% yield) at a reaction temperature of ~450 K, the ethane yield decreasing again with the further rise in bed temperature.

Ru metal. Figure 2 presents the data on the catalytic activity of polycrystalline ruthenium, evaluated under the reaction conditions mentioned above. Almost similar methane yields were obtained during injections of $CO + H_2$ (1 : 4) pulses under He or that of CO pulses under H_2 flow (Fig. 2a). As seen in these data, a measurable methane formation was observed only at the reaction temperatures above 400 K, even in the presence of excess H_2 (cf. Fig. 1). Similarly, no methane formation was detected at the catalyst temperatures below 450 K during the reaction of $CO + H_2$ (1 : 4) gas mixture under continuous flow mode. A high methane yield was, however, obtained at the reaction temperatures of 475 K and above, corresponding to a TOF of ~140×10^{-3} CH_4 molecules per site per second (Fig. 2b). Similar to the case of Ru/TiO_2, the CH_4 yield decreased rapidly after about a 15-min run in the experiment

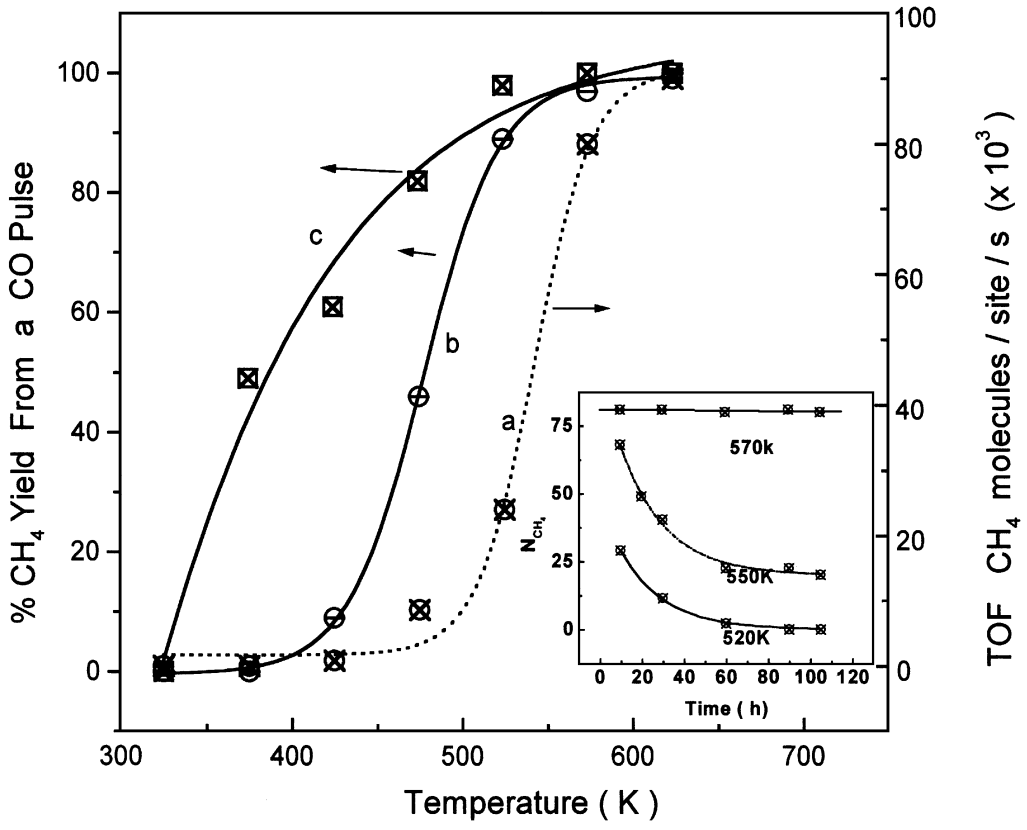

FIG. 1. CO methanation activity of Ru/TiO_2 catalyst at different temperatures and under different reaction conditions. (a) Continuous $CO + H_2$ (1 : 4) flow, (b) $CO + H_2$ (1 : 4) pulses (4.1 μmol each) dosed under He flow, and (c) 4.1-μmol CO pulses dosed under H_2 flow. (Inset) Time-dependent decay in catalyst activity when $CO + H_2$ (1 : 4) stream reacted over Ru/TiO_2 catalyst at different temperatures.

at 475 K, whereas the activity was steady for several hours of time at higher reaction temperatures.

Microcalorimetry

$CO + H_2$ Adsorption

Ru/TiO_2 catalyst. Figure 3 shows the effect of reaction temperature on the fraction of CO and H_2 adsorbed/reacted when the first $CO + H_2$ (1 : 4) pulse (4.1 μmol) was dosed over a fresh Ru/TiO_2 sample. Curve c in Fig. 3 gives the corresponding heat evolved per mole of $CO + H_2$ adsorbed. These data show that the fraction of CO adsorbed decreased progressively from a value of 62 to ~55% with the rise in exposure temperature from 300 to 470 K (Fig. 3a). On the other hand, the fraction of H_2 adsorbed/reacted increased with the rise of catalyst temperature. Thus while only ~8% of the dosed H_2 was adsorbed at 300 K, the fraction of H_2 adsorbed/reacted was found to be around 34, 40, and 50% at the reaction temperatures of 370, 420, and 470 K, respectively (Fig. 3b). As is shown in the data of Fig. 3c, around 110 kJ mol^{-1} heat was released during $CO + H_2$ exposure at 300 K. On the other hand, an almost constant $q_d = 70 \pm 5$ kJ mol^{-1} was evolved for the reaction in temperature range of 370–470 K (Fig. 3c).

When several successive $CO + H_2$ pulses (4.1 μmol each) were dosed over a catalyst sample, the amount of H_2 adsorbed/reacted from each pulse at different sample temperatures was similar to the values shown in Fig. 3b. In contrast, the fraction of CO adsorbed from successive $CO + H_2$ pulses depended on the catalyst temperature. A progressively decreasing amount of CO was adsorbed from the successive pulses at a reaction temperature of 300 K. The fraction of CO adsorbed at higher exposure temperatures, however, remained constant for the successive $CO + H_2$ pulse exposures, as shown in the data of Fig. 4.

Figure 5 gives the ratio of H_2 and CO adsorbed/reacted from the successive $CO + H_2$ pulse injections as a function of catalyst temperature. These data show that while the ratio $H_{2(ad)}/CO_{(ad)}$ increased marginally for the pulse exposures at 300 K (Fig. 5a), the values were almost constant at higher reaction temperatures.

No methane was formed during $CO + H_2$ pulse exposures at 300 and 370 K. The CH_4 yields as shown in curves e and f of Fig. 4 were, however, observed at the higher reaction temperatures. As seen in Fig. 4e, although no methane was produced during the first pulse injection at a temperature of 420 K, successive pulse injection gave rise to an increasing $CO_{(ad)} \rightarrow CH_4$ conversion, reaching an equilibrium value

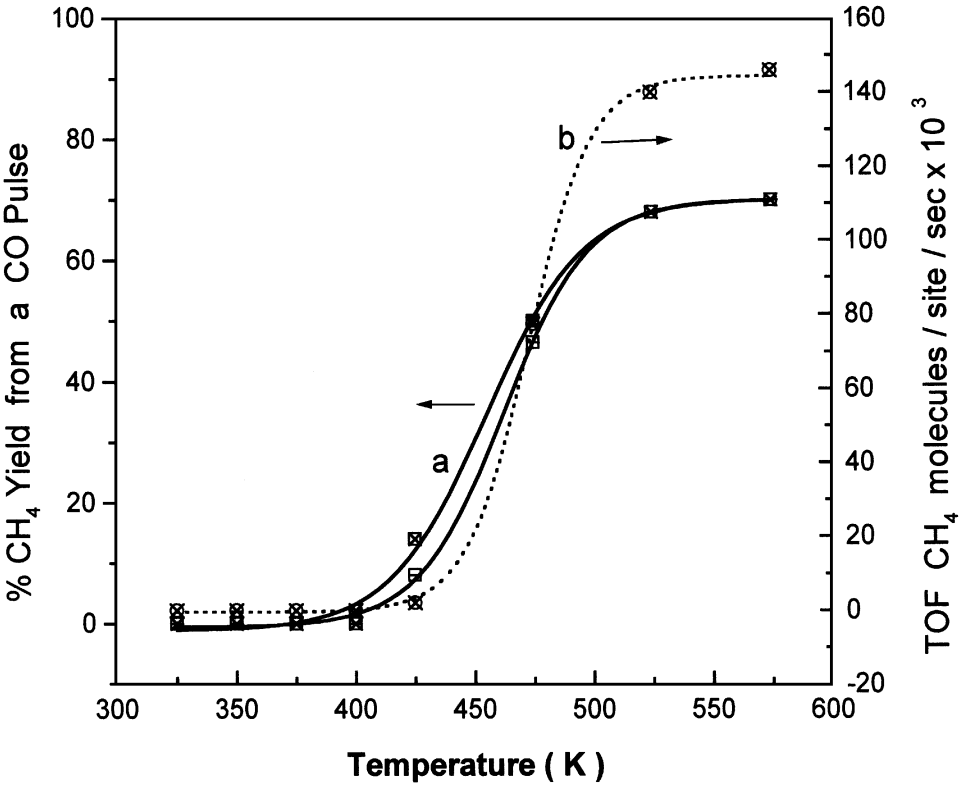

FIG. 2. CO methanation activity of polycrystalline Ru powder at different temperatures and under different reaction conditions. ⊠, Reaction of CO pulses in H_2 flow; ⊟, reaction of CO + H_2 (1 : 4) pulses under He flow; and ⊠, reaction of CO + H_2 (1 : 4) stream.

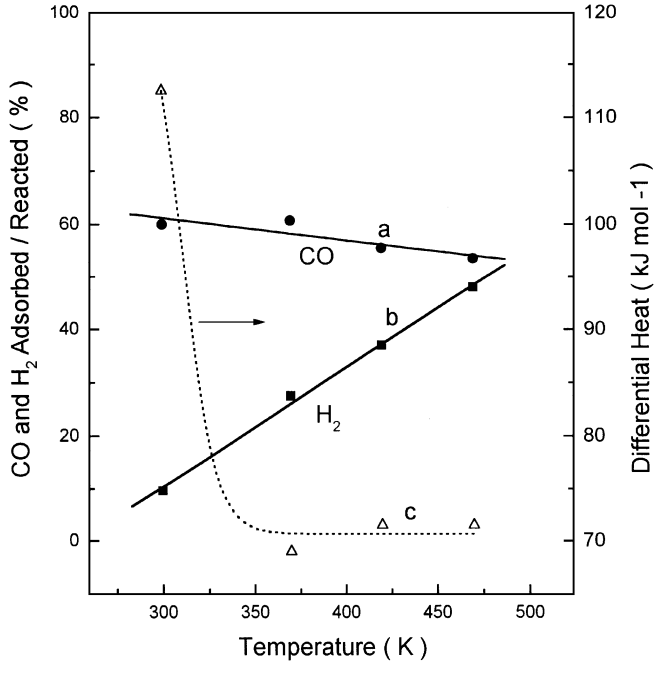

FIG. 3. Percentage of CO (curve a) and H_2 (curve b) adsorbed/reacted and corresponding differential heat evolved (curve c) when a fresh Ru/TiO_2 sample was exposed to a 4.1 μmol pulse of CO + H_2 (1 : 4) at different temperatures.

of ~33% after the fourth pulse injection. The increase in CO → CH_4 conversion during successive pulse exposures was more pronounced at a higher reaction temperature of 470 K, as seen in curve f of Fig. 4. In this case while ~8% of the adsorbed CO converted to CH_4 during first pulse injection, the yield was around 95–100% for the fourth injection onward.

The microcalorimetric data for the successive CO + H_2 (1 : 4) pulse (4.1 μmol) exposures over Ru/TiO_2 at different temperatures are included in Fig. 6. A $q_d = 110$ kJ mol^{-1} was observed when the first CO + H_2 pulse was dosed at a sample temperature of 300 K. The successive pulse exposures gave rise to lower q_d value reaching an equilibrium value of ~45 kJ mol^{-1} after the fourth pulse exposure (Fig. 6a). However, an almost constant value of heat (~70 ± 5 kJ mol^{-1}) was evolved during successive CO + H_2 pulse exposures at the sample temperatures in 370–470 K range (Fig. 6, curves b, c, and d).

Ru metal. Curves a and b in Fig. 7 show the fraction of CO or H_2 adsorbed/reacted when a fresh 100-mg ruthenium metal sample was exposed to a first 4.1-μmol pulse of CO + H_2 (1 : 4). These data show a marginal increase in the CO or H_2 adsorption with the rise in sample temperature from 300 K to 370 or 420 K and a reversal of this trend is noticed with the further rise in sample temperature. The q_d

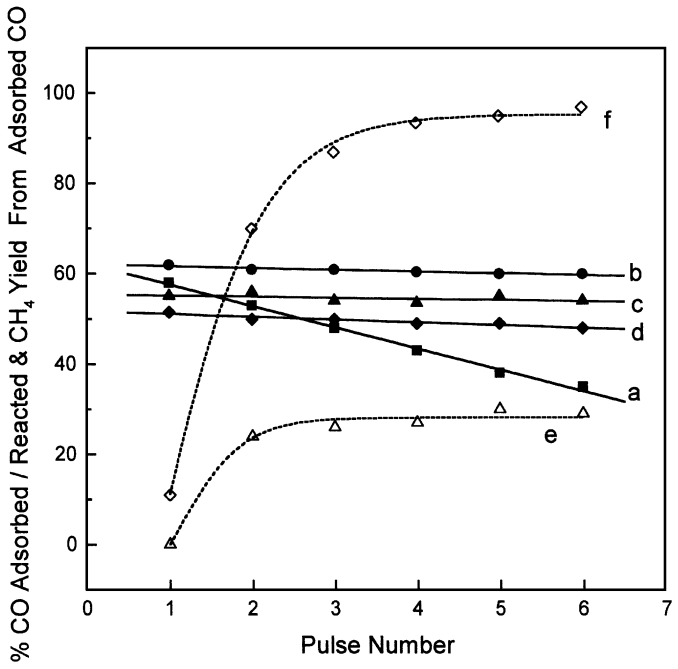

FIG. 4. Percentage of CO adsorbed/reacted (solid curves) and the yield of CH_4 from CO (dotted curves) when a Ru/TiO_2 sample was exposed to six successive pulses of 4.1 μmol $CO + H_2$ (1 : 4) at different temperatures. (a) 300 K; (b) 370 K; (c, e) 420 K; and (d, f) 470 K.

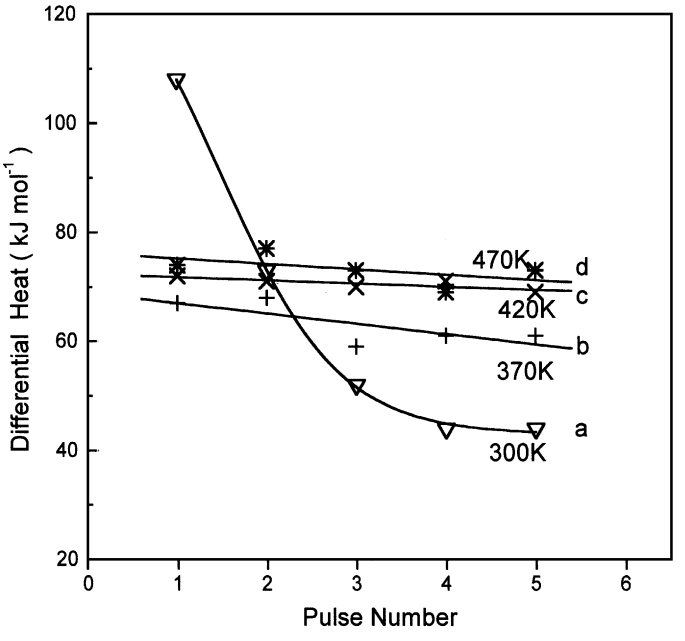

FIG. 6. Differential heat evolved during exposure of successive 4.1 μmol pulse doses of $CO + H_2$ (1 : 4) over Ru/TiO_2 catalyst at different temperatures.

values changed only marginally with the exposure temperature, the value being about 54 kJ mol^{-1} at an exposure temperature of 300 K and ~50 kJ mol^{-1} at 470 K (Fig. 7, curve c).

The data in Figs. 8 and 9 give the fraction of CO and H_2 adsorbed/reacted when a 100-mg ruthenium powder sample was exposed to six successive $CO + H_2$ (1 : 4) pulses of 4.1 μmol each at different sample temperatures. While the CO adsorption was affected only marginally (Fig. 8), the fraction of H_2 adsorbed was reduced substantially during the successive pulse exposures, the effect being more pronounced at the lower sample temperatures (Fig. 9). Thus,

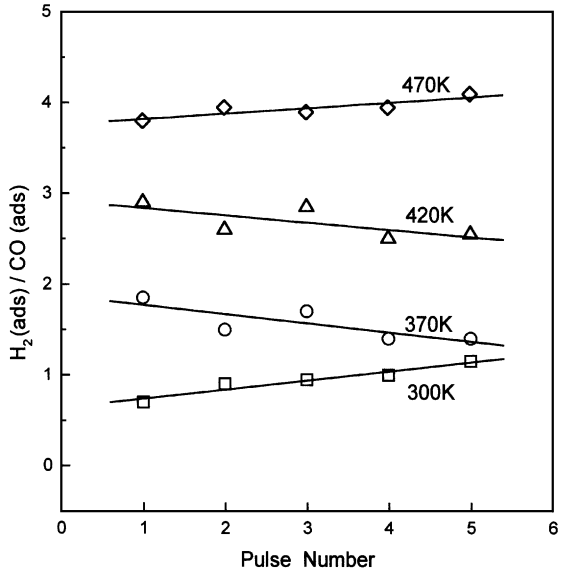

FIG. 5. Stoichiometry of H_2(adsorbed)/CO(adsorbed) on a Ru/TiO_2 sample during exposure to five successive pulse injections of 4.1 μmol $CO + H_2$ (1 : 4) at different temperatures.

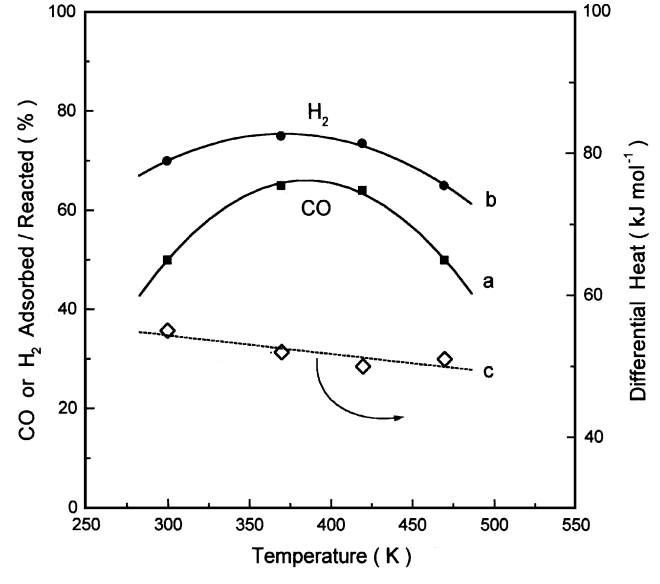

FIG. 7. Percentage of CO (curve a) and H_2 (curve b) adsorbed/reacted and corresponding differential heat evolved during exposure of polycrystalline Ru metal sample to a 4.1-μmol pulse of $CO + H_2$ (1 : 4) at different temperatures.

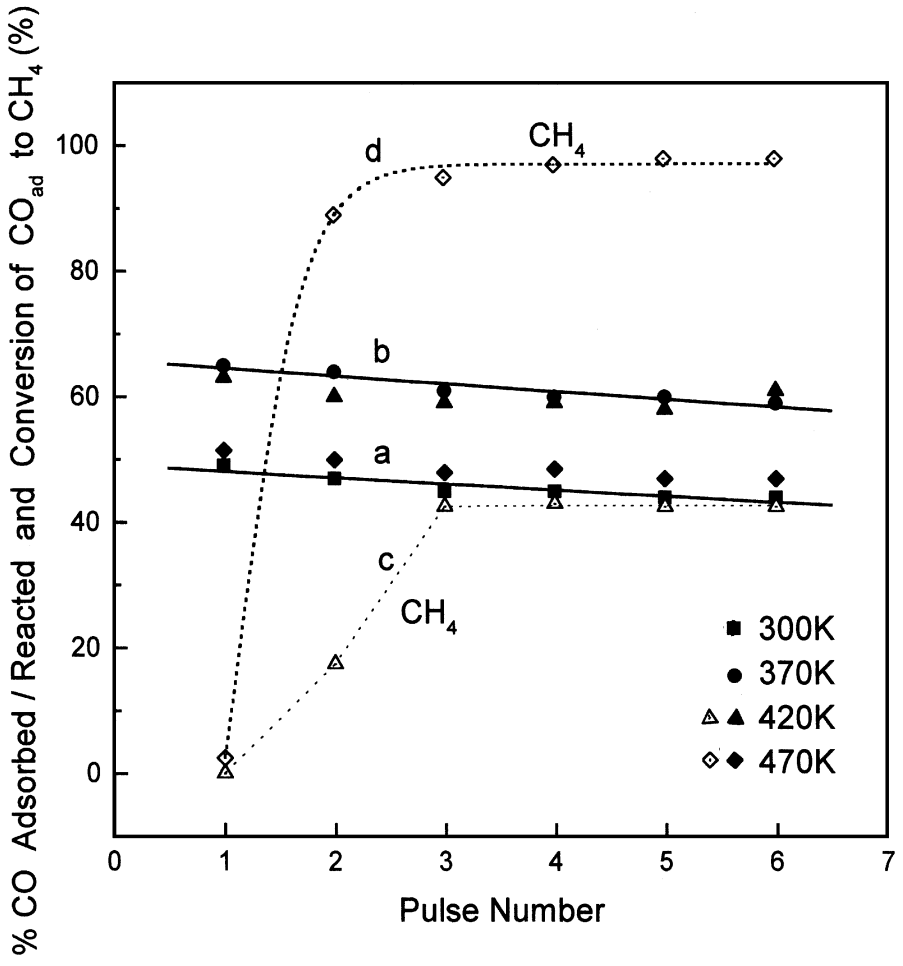

FIG. 8. Percentage of CO adsorbed/reacted (solid curves) and the conversion of adsorbed CO to methane (dotted curves) when a Ru metal sample was exposed to the successive 4.1-μmol pulses of $CO + H_2$ (1 : 4) at different temperatures.

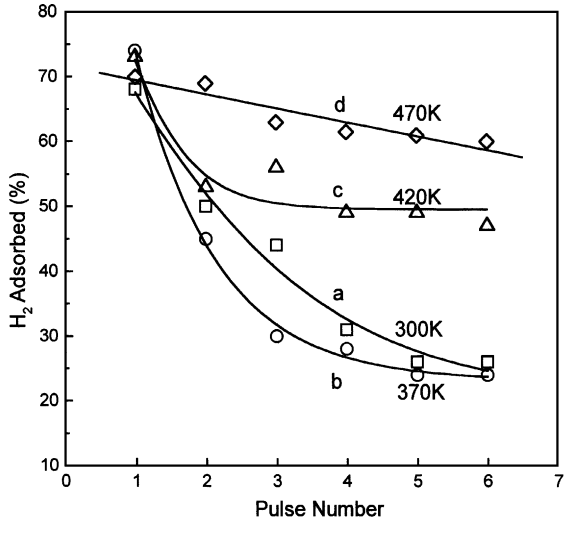

FIG. 9. Percentage of H_2 adsorbed from the successive 4.1-μmol pulses of $CO + H_2$ (1 : 4) dosed over Ru metal sample at different temperatures. (a) 300 K, (b) 370 K, (c) 420 K, and (d) 470 K.

at the exposure temperatures of 300 and 370 K the extent of H_2 adsorbed was ~70% of the dosed amount in the first pulse, the value being around 32% from the fifth and the sixth pulses. On the other hand, the H_2 adsorption at 470 K was reduced from 70% in case of the first pulse to around 62% for the sixth pulse injection (Fig. 9d). Similar to the case of the Ru/TiO_2 sample, no measurable amount of CH_4 was formed from the six $CO + H_2$ pulses dosed at the sample temperatures of 300 and 370 K. At sample temperatures of 420 and 470 K, while no CH_4 was produced from the first pulse, successive pulses gave rise to progressively increasing methane yields and the $CO_{(ad)} \rightarrow CH_4$ conversion reached a saturation value of about 45 and 98% for the reaction temperatures of 420 and 470 K, respectively. These data are given in curves c and d of Fig. 8.

Figure 10 presents the ratio of adsorbed H_2 and CO during successive $CO + H_2$ pulse exposures over ruthenium metal at different temperatures (cf. Fig. 5). The ratio $H_{2(ad)}/CO_{(ad)}$ from a 4.1-μmol $CO + H_2$ (1 : 4) pulse reduced progressively for successive pulse injections, the effect

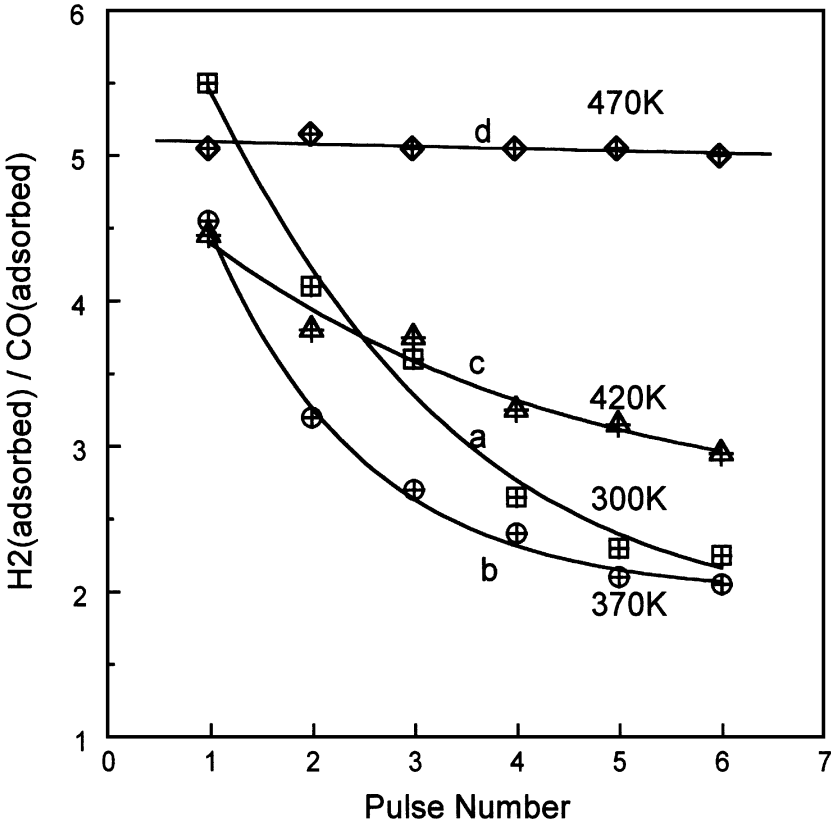

FIG. 10. Stoichiometry of H_2(adsorbed)/CO(adsorbed) on a Ru metal sample during exposure to six successive 4.1-μmol CO + H_2 (1:4) pulse doses at different temperatures. (a) 300 K, (b) 370 K, (c) 420 K, and (d) 470 K.

being more pronounced at the lower sample temperatures. Thus, while this ratio was found to reduce to 2.2 from an initial value of 5.5 for the sample temperature of 300 K (curve a), its value remained constant at ~5.1 for all the pulse injection made at 470 K (curve d).

The value of q_d remained almost constant for all the six pulses dosed at different catalyst temperatures.

The initial heat of adsorption. The q_d values at the initial stage of adsorption, as evaluated from extrapolation of log q_d vs coverage plots of the data from successive CO + H_2 pulse injections, are compiled in Table 1.

CO Adsorption in the Presence of Excess H_2

Ru/TiO_2 catalyst. Curves a and b in Fig. 11 show the fraction of CO adsorbed from the first pulse and its conversion to CH_4 as a function of catalyst temperature when the 4.1-μmol CO pulses were dosed into H_2 carrier gas flowing (20 ml min^{-1}) over catalyst bed. The corresponding amount of heat evolved is plotted in the curve c of Fig. 11. Comparing these data with those in Figs. 3 and 4 reveal that although the fraction of adsorbed CO was only marginally affected in the presence of excess H_2, the methane yields were much higher. Thus, while no methane was formed during CO + H_2 pulse injection at 370 K, the yield was ~48% in the presence of excess H_2 (Fig. 11). Similarly, against a $CO_{(ad)} \rightarrow CH_4$ conversion of ~25% from a CO + H_2 (1:4) pulse injection at 420 K (Fig. 4), the yield was ~75% when the hydrogen was available in excess (Fig. 11). Almost 100% conversion was, however, observed at the temperatures above 470 K, under both of the reaction conditions (Figs. 4 and 11). A striking difference is also noticed in the q_d values in the presence of excess H_2. While the q_d value during CO + H_2 pulse exposure was found to reduce from ~110 kJ mol^{-1} to a lower value of ~70 kJ mol^{-1} with the rise in catalyst

TABLE 1

Differential Heat (q_i) at the Initial Stage of Adsorption of CO + H_2 (1:4) over Polycrystalline Ru Metal and Ru/TiO_2 Catalyst at Different Temperatures

Catalyst temperature (K)	Ru metal (kJ mol^{-1})	Ru/TiO_2 (kJ mol^{-1})
300	56	145
370	52	68
420	50	72
470	50	74

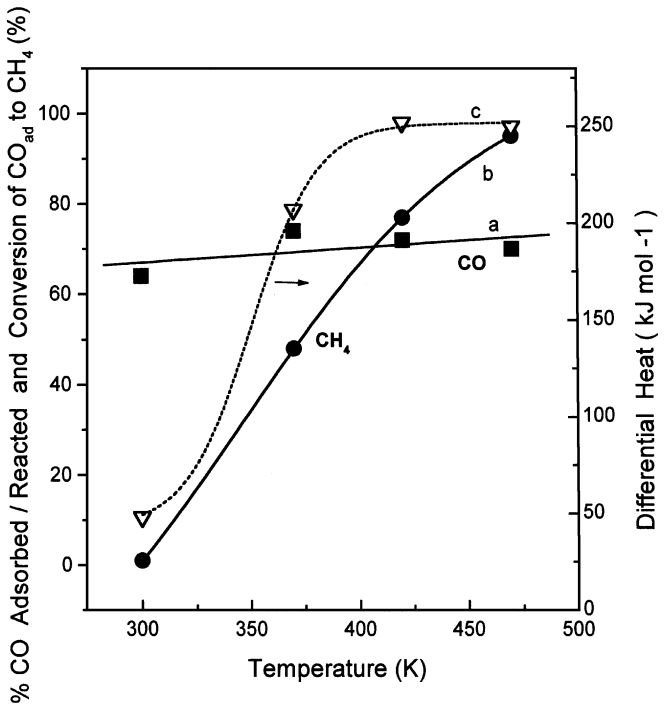

FIG. 11. Percentage of CO adsorbed/reacted (curve a) and conversion of adsorbed CO to methane (curve b) when 4.1-μmol CO pulses were reacted over Ru/TiO_2 sample in the presence of H_2 flow (20 ml min^{-1}). Curve c gives the corresponding amount of heat evolved.

temperature (Fig. 3), the trend was opposite in the presence of excess H_2 (Fig. 11c). Thus, against a value of ~50 kJ mol^{-1} at 300 K, the q_d was ~250 kJ mol^{-1} when a CO pulse was dosed in the presence of H_2 flow at 420 or 470 K (Fig. 11c).

The data similar to that shown in Fig. 11 were also obtained for all the six successively dosed CO pulses.

A comparison of the data in Fig. 11 with those on the CO adsorption over Ru/TiO_2 under helium flow (Ref. 1, Fig. 2) shows that the amount of adsorbed CO was manyfold larger when the CO pulses were introduced in the presence of H_2. The ratio of CO adsorbed in the presence of hydrogen with that of the CO adsorbed under He flow [$CO_{(H_2)}/CO_{(He)}$] is plotted in Fig. 12 for the successive pulse exposures. These data show that the $CO_{(H_2)}/CO_{(He)}$ ratio was 2.2 for the first 4.1-μmol CO pulse dosed at 300 K and this value increased to about 25 for the fifth pulse injection. This ratio, however, decreased progressively in the experiments at higher catalyst temperatures (Figs. 12b–12d). Also, the extent of this H_2-promoted adsorption of CO was marginally lower in the experiments where the $CO + H_2$ (1:4) pulses were dosed under He flow (Fig. 4). Thus, the $CO_{(H_2)}/CO_{(He)}$ ratio for the first $CO + H_2$ pulse dosed at the catalyst temperatures of 300, 370, 420, and 470 K was 1.9, 1.5, 1.3, and 1.1, respectively. The typical $CO_{(H_2)}/CO_{(He)}$ values for the successive $CO + H_2$ pulses dosed at 300 K are plotted in curve e of Fig. 12 for a comparison.

Ru metal. Figure 13 presents the data on the fraction of CO adsorbed and its conversion to CH_4 when the first CO pulse was dosed over polycrystalline Ru in the presence of H_2 flow (20 ml min^{-1}) and at different reaction temperatures. Again, about 60–65% of the dosed CO was adsorbed, the amount increasing marginally with the rise in sample temperature (Fig. 13a). A striking difference between the data in Figs. 11 and 13 lies in the commencement of CO methanation at a higher reaction temperature in the case of Ru metal under identical reaction conditions. Thus, as also observed in Fig. 2, while no methane was produced using bulk Ru at the reaction temperatures up to 400 K, the yield at 420 K was only ~14% (Fig. 13). The q_d values were also different, the differential heat being 80–90 kJ mol^{-1} at 300 and 370 K and ~175–190 kJ mol^{-1} at the higher reaction temperatures (cf. Fig. 11).

The fraction of adsorbed CO reduced progressively for the successive CO pulse injections, the effect being more pronounced at reaction temperatures below 400 K. The methane yield was, however, found to be constant for all the CO pulse injections made under this test condition. In line with the reduced amount of adsorbed CO at the exposure temperatures of 300 and 370 K, the q_d values were found to reduce for the successive pulse injections, reducing from an initial value of 80 kJ mol^{-1} to a value of ~30 kJ mol^{-1} after the fifth pulse injection made at 300 K.

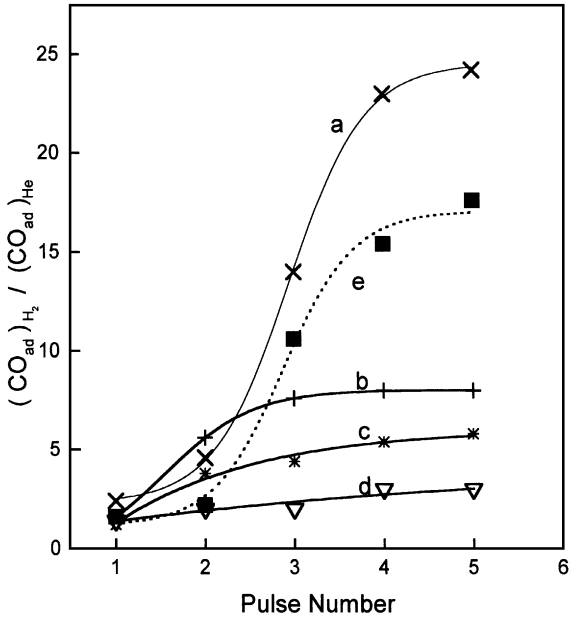

FIG. 12. The ratio of CO uptake in presence of H_2 flow to the uptake in presence of He flow when successive 4.1-μmol pulses of CO were dosed over Ru/TiO_2 catalyst at different temperatures. (a) 300 K, (b) 370 K, (c) 420 K, and (d) 470 K. Curve e shows similar ratio of CO adsorbed from successive $CO + H_2$ (1:4) pulses and from pure CO pulses dosed over Ru/TiO_2 under He flow and at a temperature of 300 K.

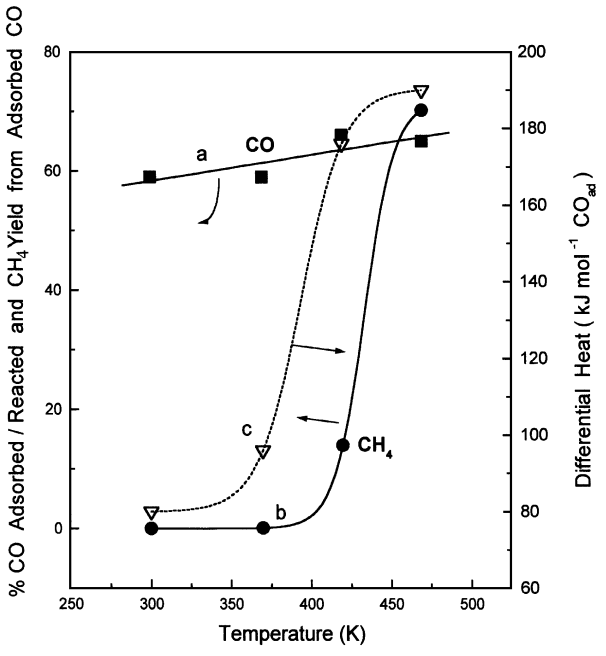

FIG. 13. Percentage of CO adsorbed/reacted (curve a) and the conversion of adsorbed CO to CH_4 (curve b) when a Ru metal sample was exposed to 4.1-μmol CO pulses under hydrogen flow (20 ml min^{-1}) at different temperatures. Curve c shows the corresponding amount of differential heat evolved.

In contrast to the data of Fig. 12, $CO_{(H_2)}/CO_{(He)}$ values in the case of Ru metal were almost constant at 1.1 ± 0.2 for the CO pulse exposures in presence of H_2 or the $CO + H_2$ (1 : 4) pulse exposures in He flow, as observed for the four to five pulses dosed a different temperatures.

FTIR Spectroscopy

FTIR spectra of Ru/TiO_2 catalyst exposed to 100 Torr $CO + H_2$ (1 : 4) at different temperatures are compiled in Fig. 14. The room temperature adsorption gave rise to CO stretch region bands appearing at frequencies 2185, 2144, 2085, 2045, and 2010 cm^{-1}, in addition to the IR bands due to adsorbed CO_2 (2350–2400 cm^{-1}) and certain oxygenated species (1100–1800 cm^{-1} bands). The adsorption of $CO + H_2$ at elevated temperatures resulted in the removal of oxygenate species as well as νCO_2 bands in 2350–2400 cm^{-1} region and at the same time gave rise to the new C–H stretch region bands at 2856 and 2930 cm^{-1} (Fig. 14c). With the further rise in catalyst temperature to 470 K, the methylene group bands progressively gave way to methane formation. The relative intensity of various C–O stretch region bands also underwent a considerable change with the rise in exposure temperature. This becomes clear from the deconvolution of νC–O bands in the IR spectra of Ru/TiO_2 exposed to 100 Torr $CO + H_2$ (1 : 4) at different temperatures, as is shown in Fig. 15. Spectra a–d in this Fig. 15 show that at the sample temperatures of 370 K and above, the 2144 cm^{-1} band shifted to 2138–2135 cm^{-1} and its intensity reduced marginally. On the other hand, a new band was observed at 2105 cm^{-1}, its intensity increasing with the rise in temperature (Figs. 15b and 15d). The band at 2085 cm^{-1} shifted to 2072 cm^{-1} at elevated temperatures and its intensity appeared to be coupled with that of a new band at 2105 cm^{-1}. Other noticeable changes in these spectra are almost complete removal of 2045 cm^{-1} band which showed a red shift of $\sim$15 cm^{-1} and the significant growth of a band at 2000 cm^{-1} (Fig. 15d), which was observed at 2010 cm^{-1} in the room temperature spectrum (Fig. 15a). The results of detailed IR study on the effect of metal dispersion and of exposure temperature on the adsorption of CO and $CO + H_2$ over Ru/TiO_2 sample used in this study are given elsewhere (5).

DISCUSSION

Adsorption

The data plotted in Fig. 12 show that the CO uptake by Ru/TiO_2 was enhanced considerably in the presence of H_2, the extent of which depended on the factors such as catalyst temperature, ratio of H_2/CO in the adsorbate, and the surface coverage. Similar results have been reported earlier for Ru and other transition metals. For instance, Miura *et al.* (7) found a 2.8-fold increase in the total CO chemisorption over Ru/SiO_2 catalyst due to preadsorbed H_2. This increase was attributed to the reconstruction of the CO adlayer because of the presence of coadsorbed H_2. These authors have also suggested that a surface complex between CO and hydrogen is an unlikely explanation for this phenomenon (7). Wedler *et al.* (8) showed that in the presence of H_2 the capacity of Ni films for CO uptake at 353 K was two times higher than the uptake of CO on clean Ni films. No increase in CO adsorption due to H_2 presence was, however, observed in their study at 273 K.

Our study, on the other hand, shows that unlike in the case of Ru/TiO_2, no H_2-induced enhancement in CO adsorption was observed using Ru metal at all the temperatures under this study and the fraction of CO adsorbed was almost similar when a pulse of CO or $CO + H_2$ (1 : 4) was dosed over Ru metal (cf. Fig. 4, Ref. 1). The data given in Figs. 3 and 7 reveal that the chemisorption behavior of bulk Ru and Ru/TiO_2 is quite different from each other, when exposed to a dose of $CO + H_2$ (1 : 4) under identical conditions. The Ru/TiO_2 was more selective to CO chemisorption, particularly at low temperatures. Thus, even though H_2/CO molar ratio in the dosed pulse was 4, only $\sim$9% of the H_2 was held over Ru/TiO_2 at 300 K (Fig. 3b) compared to a 60% fraction of the injected CO (Fig. 3a). Also, while the fraction of H_2 adsorbed increased with the rise in catalyst temperature, the amount of adsorbed CO decreased only marginally. On the other hand, these gases were adsorbed over Ru metal in almost same CO/H_2

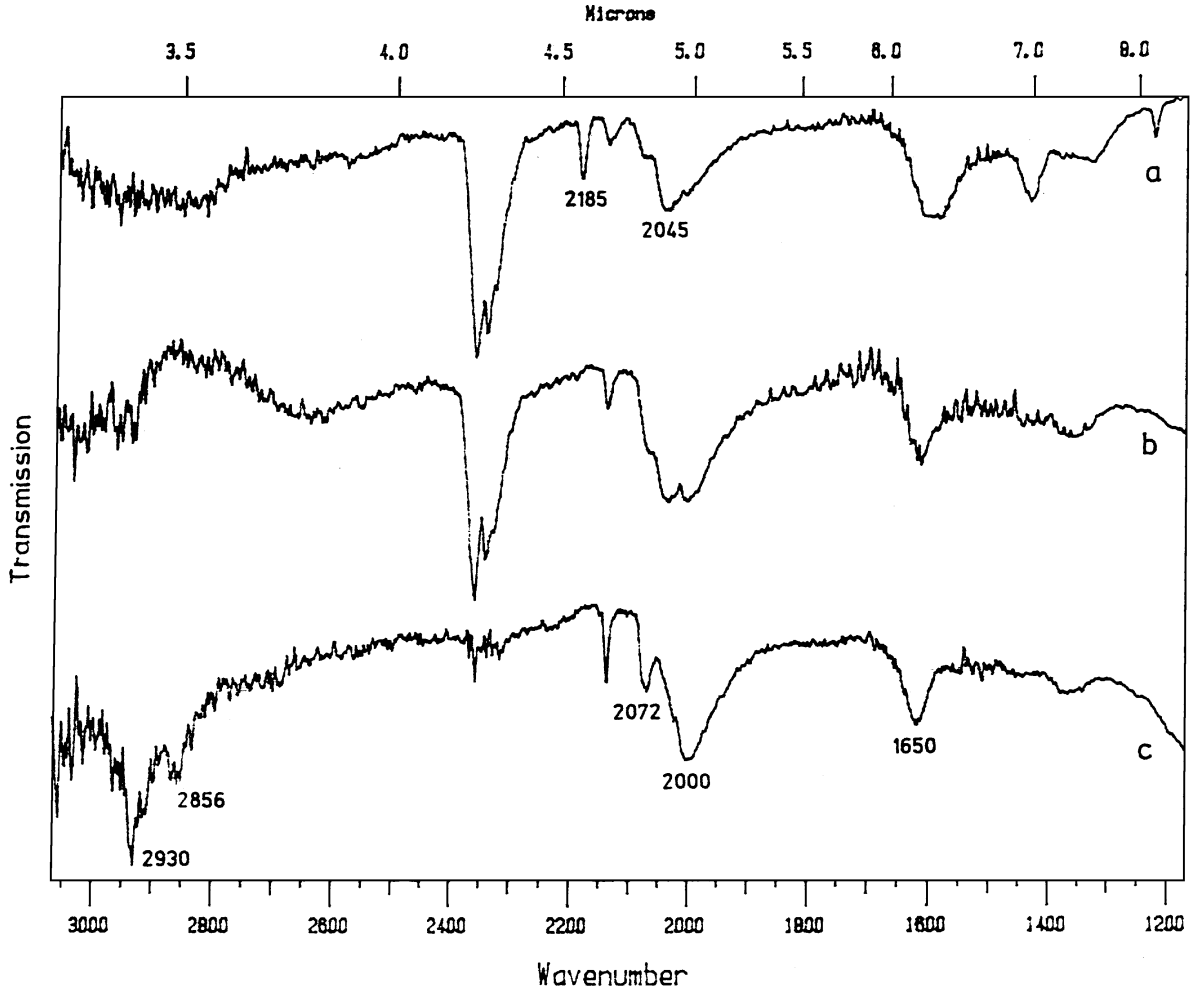

FIG. 14. FTIR spectra of Ru/TiO_2 wafer after exposure to 100 Torr $CO + H_2$ (1:4) at different sample temperatures. (a) 300 K, (b) 370 K, and (c) 420 K.

ratio at all the catalyst temperatures under study (Figs. 7a and 7b).

These observations can be understood in the light of FTIR results given in Figs. 14 and 15. The assignments to different C–O stretch region bands in these Figs. 14 and 15 are discussed in our earlier publications (1–5) and are also reviewed by other authors (9, 10). A band appearing at 2185 cm^{-1} is removed easily at elevated temperatures (Fig. 15b) or under vacuum and is generally attributed to the physically adsorbed CO. While the νCO bands in 1900–1950 cm^{-1} region are attributed to the bridge-bonded CO, the 1950–2050 cm^{-1} region bands are assigned to the linearly bonded CO at a Ru cluster site (Ru_xCO), where $x = 2$ or more. On the other hand, the higher frequency bands in 2140–2050 cm^{-1} region are believed to arise from the multicarbonyl ($M(CO)_n$, $n = 2$, 3) species bonded to highly dispersed Ru sites of different oxidation states. Thus, a pair of bands appearing at 2140 and 2085 cm^{-1} is identified with such species associated with the zero-valent Ru, whereas the pair of bands at 2135 and 2080 cm^{-1} is assigned to $M^{\delta+}(CO)_n$ structures, where $M^{\delta+}$ represents the metal sites of higher oxidation state. The spectra in Figs. 14 and 15 show the presence of prominent νCO bands at 2144, 2085, and 2045 cm^{-1} in addition to a weak shoulder peak at around 2010 cm^{-1}. As discussed above, the band at 2144 cm^{-1} (along with 2085 cm^{-1} band) may be identified with the $Ru^{\circ}(CO)_n$ type surface species. At higher exposure temperatures, the 2144 cm^{-1} band shifted to a lower frequency of 2135 cm^{-1} and its intensity (area under the peak) reduced marginally. At the same time, a new band appeared at 2105 cm^{-1}, the intensity of which increased with the rise in catalyst temperature (Figs. 15b– 15d). The growth of 2105 cm^{-1} band was accompanied by the growth of a band peaking at 2071 cm^{-1} which perhaps overlaps with a 2085 cm^{-1} band of low intensity (Figs. 15c and 15d). The 2071 and 2105 cm^{-1} bands may thus be considered to be the coupled vibrations arising from a single species. In accordance with the arguments given in Refs. (9) and (10),

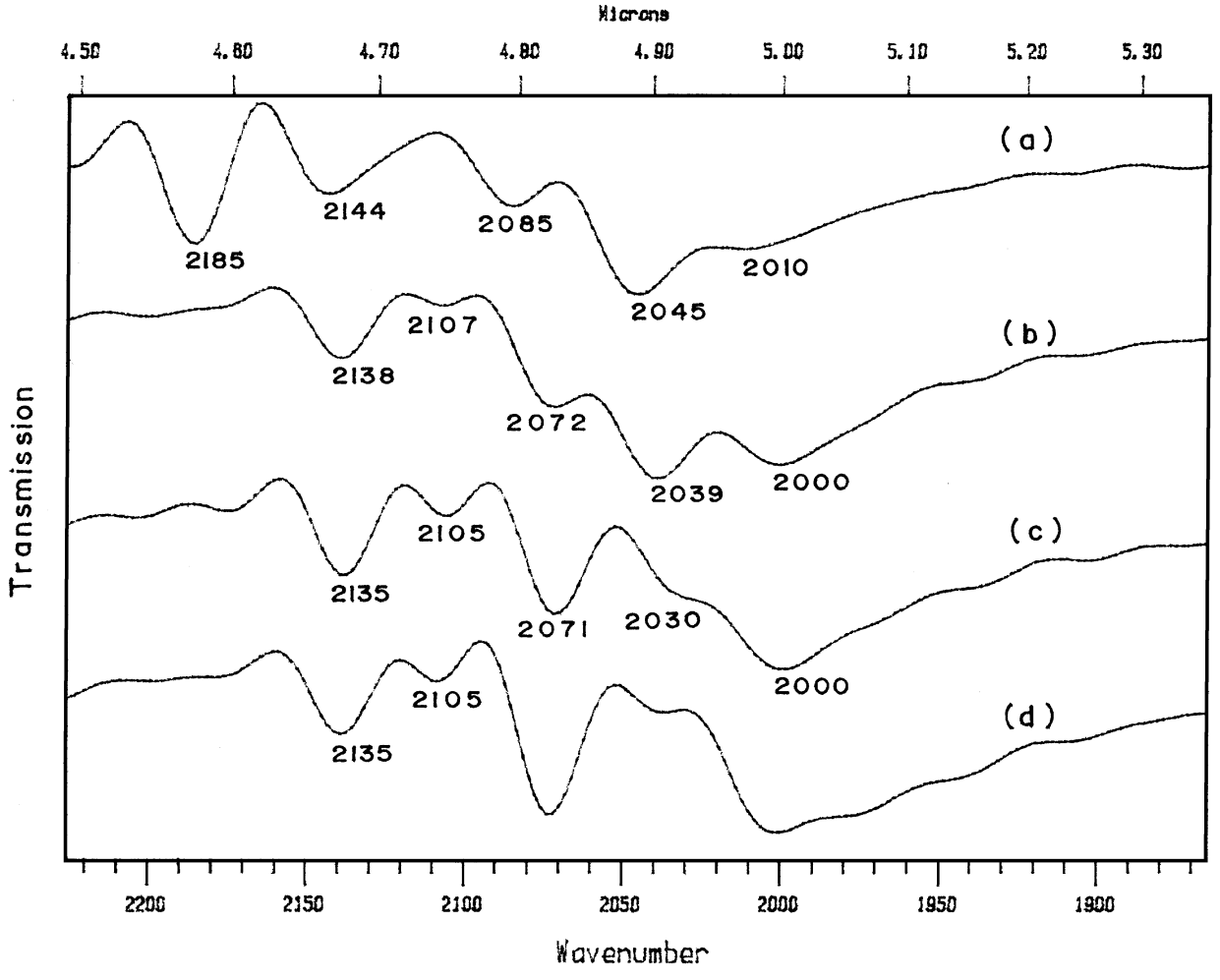

FIG. 15. Deconvolution of C–O stretch region bands developed over Ru/TiO_2 wafer during exposure to 100 Torr $CO + H_2$ (1:4) at different temperatures. (a) 300 K, (b) 370 K, (c) 420 K, and (d) 470 K.

we assign the 2135 and 2085 cm^{-1} bands to

$$\mathrm{Ru}\begin{matrix}\diagup\,\mathrm{H}\\ \diagdown\,(\mathrm{CO})_n\end{matrix}$$

structure and the bands at 2105 and 2071 cm^{-1} to

$$\mathrm{Ru}\begin{matrix}\diagup\,\mathrm{H}\\ \diagdown\,(\mathrm{CO})_{n-1}\end{matrix}$$

species, where $n = 2$ or 3. Since these bands appeared even after a prolonged hydrogen pretreatment given to a catalyst *in situ*, their assignment to hydrocarbonyl rather than the oxycarbonyl type coadsorbed species seems to be more tenable, particularly in the case of the data of present study. These assignments are consistent with the observations that the presence of an electropositive additive on the metal surfaces resulted in the lowering of C–O stretching frequency of the coadsorbed CO. This is also in agreement with the study of King (11), who demonstrated that an IR band appearing at 2045 cm^{-1} after adsorption of CO over silica- and alumina-supported Ru shifted to 2020 cm^{-1} when the H_2 was coadsorbed. From the shifts in IR spectra, he concluded about the existence of H_2–CO interaction which weakens the CO bond and also showed that this weakly held CO is more reactive since its intensity decreased under reaction conditions. Another noticeable feature of the data in Figs. 14 and 15 is the progressive decrease in the intensity of 2045 cm^{-1} band and a simultaneous growth of the low frequency band at 2000 cm^{-1} as a function of increase in the exposure temperature. In addition, the presence of new and strong bands at around 1940 and 1970 cm^{-1} is also indicated in spectra c and d of Fig. 15 which possibly indicate the formation of new bridge-bonded CO adstates at higher sample temperatures.

We can therefore conclude that some of the species giving rise to the high frequency bands are unstable and they transform to other more stable forms. From the relative intensity of various IR bands in Fig. 15, we thus infer that

while the number of $MH(CO)_n$ surface species reduces, the $MH(CO)_{n-1}$ and $M_x(CO)$ species grow at the elevated temperatures. This finds a support in our study reported in Ref. (2) on a better dispersed Ru/TiO_2 catalyst, where it was shown that the multicarbonyl species transform to a monocarbonyl form at elevated temperatures which in turn give rise to formation of a methylene group chain to serve as methane precursor. The presence of hydrogen is found to promote this process. The lowering of C–O stretch frequency from 2144 to 2135 and 2105 cm^{-1} (Fig. 15) is an evidence for the C–O bond weakening.

On the contrary, no multicarbonyl type surface species are known to develop on the adsorption of CO over single crystal or polycrystalline forms of noble metals, including Ru, as is reviewed in various articles (12–15). A CO molecule is known to bond with bulk transition metals either at a single metal site in linear form (M–CO) or at more than one sites in a bridged (M_2=CO) or multiply bonded (M_3≡CO) forms. For instance, the CO adsorbed on Ru(001) surface is reported to exist in a single binding state giving rise to IR vibrational band at 1984 cm^{-1}, the frequency of which increased with the surface coverage (16). Williams and Weinberg (17) showed that depending on surface coverage the CO may adsorb on Ru(001) at 110 K occupying either the "on top" or the bridging sites.

The following picture thus emerges from the observations made above. In the case of dispersed Ru, the nature of CO binding states depends upon the catalyst temperature. At lower temperatures, a significant fraction of CO is held in form of multicarbonyls which may sterically hinder hydrogen adsorption, as is reflected in the data of Fig. 3. The transformation of some of these complexes to mono- or bridge-bonded carbonyls (Fig. 15) would change the $CO(ad)/H_2(ad)$ stoichiometry at elevated temperatures, which is in agreement with the adsorption data in Fig. 3. In the case of polycrystalline Ru, CO adsorbs only in the linear form thus showing uniform CO/H_2 stoichiometry of adsorbed gases at different temperatures (Fig. 7).

Various research groups have reported that the mode and the stoichiometry of CO adsorption over a noble metal surface depends on its dispersion (18–20). The metal crystallites of large size are known to adsorb CO in the bridged or in the linear form giving rise to the Ru_xCO type species. On the other hand, the well-dispersed metal sites are responsible to the formation of multicarbonyl species (18–20). The recent IR studies have demonstrated that the adsorption over supported ruthenium results in the oxidative disruption of Ru_x clusters and hence in the growth of $Ru(CO)_n$ type surface species (9, and references cited therein). It has also been demonstrated that at high temperatures the reductive agglomeration of Ru crystallites took place, which gave rise to the growth of Ru_x clusters. The progressive growth of the 1900–2000 cm^{-1} region vibrational bands in Fig. 15 is in agreement with these findings.

Heat Values

The differential heat evolved during the first $CO + H_2$ (1 : 4) pulse exposure (Figs. 3 and 7) (q_{exp}) is found to be different from the q_d values calculated (q_{cal}) on the basis of the amount of CO and H_2 adsorbed on the catalyst surface and the heat evolved during their individual adsorption (Ref. 1). In the case of Ru/TiO_2, the experimental q_d values were generally higher than the q_{cal} values. On the contrary, the q_{exp} values in the case of Ru metal were marginally lower than the q_{cal}. Table 2 presents a comparison of these data. Since no methane formed at 300 K, the $q_{exp} \sim 117$ kJ mol^{-1} for the $CO + H_2$ (1 : 4) exposure over Ru/TiO_2 at this temperature, compared to the corresponding $q_{cal} \sim 80$ kJ mol^{-1} (Table 2), indicates the influence of an exothermic step in addition to the adsorption of CO and H_2 at metal sites. This exothermic step could be identified with either the formation of surface complexes as discussed above or a disproportionation reaction, i.e.,

$$2CO \rightarrow C_s + CO_2, \quad \Delta H = -172 \text{ kJ mol}^{-1}$$

This reaction, however, has an energy barrier due to high activation energy requirement for CO dissociation ($\sim$300 kJ mol^{-1}) (12) and also since no measurable CO_2 was detected in the effluents during $CO + H_2$ pulse exposures at 300 K, we conclude that the formation of surface complexes with the coadsorbed CO and H_2, as discussed above, contribute significantly to q_{exp} values. The reduced number of some of these surface complexes (Figs. 15b–15d) may explain a smaller gap between the q_{exp} and the q_{cal} values for the $CO + H_2$ adsorption over Ru/TiO_2 at higher catalyst temperatures (Table 2).

In a calorimetric study of coadsorption of hydrogen and carbon monoxide over ruthenium-graphitized carbon black catalysts, Querrero-Ruiz (21) attributed the observed enthalpy values to H_xCO complex formation. The nature of this complex was found to depend on the surface coverage of H_2 or CO.

TABLE 2

Heat Evolved (kJ mol^{-1}) during Adsorption of a 4.1-μmol $CO + H_2$ (1 : 4) Pulse over Fresh Ru/TiO_2 and Ru Metal Catalysts at Different Temperatures

	Ru/TiO_2		Ru metal	
Temperature (K)	Calculated from amounts of CO and H_2 adsorbed	Experimental value	Calculated from amounts of CO and H_2 adsorbed	Experimental value
300	76.9	117.0	54.0	53.1
370	63.4	67.0	56.5	51.2
420	57.4	72.8	56.9	48.6
470	51.2	72.2	53.5	50.0

In contrast to Ru/TiO_2, a close proximity between the two q_d values in the case of Ru metal (Table 2) indicates the adsorption of both the adsorbates at distinct metal sites. The marginally lower q_d values observed at the higher reaction temperature could be attributed to the contribution of a slightly exothermic process involving CO dissociation, i.e., $CO_{ad} \rightarrow C_s + O_s$, ($\Delta H = \sim -8$ kJ mol^{-1}, $\Delta E =$ 300 kJ mol^{-1}).

The microcalorimetric data in Figs. 3, 6, 7, and 11 reveal that the q_d values are by and large governed by the initial steps involved in the interaction of CO and H_2 at metal sites and not by the subsequent transformations occurring over catalyst surface; viz. $C_s + xH_s \rightarrow CH_{x(ad)} \rightarrow CH_{4(g)}$. These data also reveal that the interaction of CO with the titania support plays an insignificant role in the presence of H_2, even at the elevated temperatures (cf. Ref. 1).

We now come to the q_d values in Fig. 11 concerning CO adsorption over Ru/TiO_2 in the presence of flowing H_2. A $q_d \sim 50$ kJ mol^{-1} evolved during CO pulse exposures at 300 K indicates the predominant surface coverage by H_2 ($q_d \sim 45$ kJ mol^{-1}, Fig. 6, Ref. 1), even though about 60% of the dosed CO from a pulse was adsorbed (Fig. 11a). At the reaction temperature of 370 K and above, the q_d value was in the range 200–250 kJ mol^{-1} (Fig. 11c) compared to the lower value of ~70 kJ mol^{-1} observed for the $CO + H_2$ (1 : 4) pulse exposures under identical conditions. Though the fraction of CO adsorbed remained the same (~60–70%) (Figs. 3a and 11a), the excess H_2 had direct bearance on the CH_4 yield under the two different reaction conditions. Thus, while the conversion of adsorbed CO to CH_4 in the presence of excess H_2 is around 50 and 80% at reaction temperatures of 370 and 420 K, respectively (Fig. 11b), the methane yields were 0 and 30% when $CO + H_2$ (1 : 4) pulses were dosed under similar conditions (Fig. 4). These data thus indicate that the concentration of hydrogen around C_s species at the time of its formation over catalyst surface plays a decisive role in the catalyst activity. The high q_d values of ~200–250 kJ mol^{-1} in Fig. 11 may therefore be attributed to the increasing contribution of a step, viz.

$$C_s + 4H_{(ad)} \rightarrow CH_4$$

In the case of $CO + H_2$ (1 : 4) pulse injections, the activity of C_s species may decay rapidly. This is reflected well in the fall of catalyst activity during continuous flow experiments, particularly at low reaction temperatures (Fig. 1, inset). The deactivation of nascent C_s species formed during dissociation of CO over group VIII metals is now a well-known phenomenon, as is reviewed by various authors (for an example, see Ref. 13).

Effect of Surface Coverage

The effect of surface coverage on CO adsorption over Ru/TiO_2 is different when the sample was dosed with $CO + H_2$ or pure CO, as is also reflected in the data of Fig. 12. These data show that the $CO_{(H_2)}/CO_{(He)}$ ratio increased progressively for the successive 4.1-μmol CO pulses the effect being more pronounced in the case of low sample temperatures (Figs. 12a–12c). These results may be explained by the progressive poisoning of catalyst surface due to either $M(CO)_x$ type complexes at low exposure temperatures or carbidic species formed during the disproportionation/dissociation of CO at elevated temperatures, the effect being more pronounced in the absence of hydrogen. These results again confirm the promotional effect of hydrogen in the desorption/disproportionation of CO as discussed above. This also becomes evident from the comparison of the data for the successive pulse exposures of $CO + H_2$ (Fig. 4) with that of the corresponding pure CO pulse injections (Fig. 2, Ref. 1).

The data in Fig. 8 show an almost similar CO uptake from the successive $CO + H_2$ pulses dosed over Ru metal at different temperatures, while in the absence of hydrogen a progressive loss in CO uptake was observed (cf. Fig. 4, Ref. 1). This again reveals the weakening of CO bonding at metal sites in the presence of H_2. The data in Figs. 9 and 10 show that the progressive increase in the CO surface coverage blocked the hydrogen chemisorption sites, the effect being more pronounced at lower sample temperatures (Figs. 10a and 10b). However, after the sixth $CO + H_2$ pulse exposure an equilibrium stoichiometry of $H_{2(ad)}/CO_{(ad)} = 2$–3 was observed for the reaction temperatures of 300–420 K (Figs. 10a–10c), even under those conditions where CO methanation was not detected (Fig. 8). These observations thus reveal the heterogeneity of the hydrogen adsorption sites and show that some of the metal sites are less prone to C poisoning.

Methane Formation

The data in Figs. 1, 4, and 11 show that no significant amount of methane was produced when $CO + H_2$ (1 : 4) reacted in flow mode at the temperatures below 475 K (Fig. 1a). On the other hand, about 8 and 60% of the adsorbed CO was methanated when 4.1 μmol of $CO + H_2$ (1 : 4) or 4.1 μmol CO in H_2 flow, respectively, were reacted at 420 K in the pulse form (Fig. 1c). It is also of interest to note that a high $CO_{(ad)} \rightarrow CH_4$ conversion was observed at the reaction temperatures as low as 350 K (10–30%) and 370 K (~50%) using Ru/TiO_2 catalyst in the presence of excess H_2 (Figs. 1c and 11b). In the case of Ru metal, a measurable amount of CH_4 was detected only at the reaction temperatures above 400 K, under all the studied reaction conditions (Figs. 2 and 13b).

We may therefore conclude that the reaction routes followed in the CO methanation could be different in the cases of the supported and the bulk forms of ruthenium metal. As discussed above, the $Ru(CO)_n$ species are formed on

a well-dispersed metal surface (Figs. 14 and 15). Some of these structures are unstable and transform to the linear or bridge-bonded species at higher reaction temperatures and the process is facilitated in the presence of hydrogen. In the absence of H_2, they block some Ru sites and hinder CO and H_2 adsorption, particularly at low temperatures (see Ref. 1). We, therefore, infer that the formation of the multicarbonyls and their transformation/decomposition in the presence of H_2 may control the methanation reaction over Ru/TiO_2 at lower reaction temperatures. The studies using metal single crystals for varying surface coverages have shown that the flat lying or the strongly inclined CO configurations dissociate with ease on heating compared to the CO bonded in Blyholder-type configuration, i.e., CO axis normal to the metal surface (22–24). For example, in a high resolution electron energy loss spectroscopy study, it has been demonstrated that the inclined CO adsorbed over Mo(110) surface showing a low-frequency νCO band at 1345 cm^{-1} converted to C and O via an excited intermediate CO^* state characterized with $\nu CO = 1130$ cm^{-1} at a temperature as low as 200 K (12). It has thus been established that in the favorable CO bonding configurations, the C–O bond scission could be achieved at fairly low temperatures.

Taking a clue from these single crystal studies we can therefore infer that the CO bonded in form of multicarbonyls may be more susceptible to C–O bond scission and may have lower dissociation energy requirement than that of the linearly bonded CO. The formation of CH_4 at low temperatures (<400 K) (Figs. 1 and 11) may thus be attributed to these multicarbonyl species.

The CO adsorbed over large Ru crystallites in the bridged or linear form may behave in a way similar to that of CO adsorbed over bulk Ru. The CO methanation in these cases may occur only at high temperatures (Fig. 13), when the activation energy requirements are presumably met. It may therefore be surmised that the CO methanation at higher temperatures followed a $CO_{(ad)} \rightarrow C_s \rightarrow CH_4$ route. The progressive increase in CH_4 yield for the first few $CO + H_2$ pulses dosed over both the Ru/TiO_2 and the Ru metal samples (Figs. 4 and 8) is in agreement with a view that a similar multistep route via active carbon formation is followed in the cases of the two catalysts at high reaction temperatures.

Another important observation of this study pertains to the rapid poisoning of the catalytic activity at lower reaction temperatures while the activity at the temperatures above 470 K was found to be stable during several hours of study. This is contrary to the expected behavior of "active" carbidic–carbon → graphite transformation, which is expected to be more prominent at higher catalyst temperatures. We, therefore, attribute this behavior to $Ru–(C)_x$ type species formed during the dissociation of multicarbonyls which may graphitize at a rate faster than the single carbon species formed from linear form of CO bonding. The referee has opined that the formation of carbonyls could give rise to a restructuring of the metal surface and cause the type of deactivation that we observe at low temperatures. Though such a possibility cannot be completely ruled out, it may be difficult to visualize a large scale surface restructuring during adsorption at temperatures below 475 K resulting in a drastic loss in low temperature catalytic activity as shown in Fig. 1.

Our views are supported by the findings of our recent studies (5) where we demonstrated that a H_2 pretreatment given to Ru/TiO_2 above 670 K resulted in the inhibited formation of the multicarbonyl species during $CO + H_2$ (1 : 4) exposure and this showed a parallelism with the substantial agglomeration of Ru at the catalyst surface and also the loss of the catalyst activity only at the reaction temperatures below 450 K. The catalyst activity at higher reaction temperatures (>550 K) and the linearly bonded CO adstates (~2000 cm^{-1}) remained by and large unaffected by the high-temperature H_2 pretreatment given to a catalyst wafer prior to $CO + H_2$ exposure.

SUMMARY

Following conclusions may be drawn from this study.

1. The CO uptake by a Ru/TiO_2 catalyst increased several fold in the presence of coadsorbed H_2. The extent of H_2-promoted CO adsorption depended on various factors such as the catalyst temperature and the surface coverage. No such enhancement was observed during the coadsorption of CO and H_2 over polycrystalline metal surface at different temperatures in the range 300–470 K. Thus, the stoichiometry of CO/H_2 adsorbed were quite different when $CO + H_2$ were adsorbed over Ru/TiO_2 and bulk Ru metal at different temperatures. In the case of Ru/TiO_2, only a small fraction of H_2 was adsorbed at room temperature and the ratio of $H_{2(ad)}/CO_{(ad)}$ increased progressively with the rise in catalyst temperature. In the case of Ru metal, the ratio $H_{2(ad)}/CO_{(ad)}$ was ~1 at all the exposure temperatures.

2. The adsorption and FTIR data indicate the formation of $Ru(CO)_n$, $RuH(CO)_n$, and Ru_xCO complexes, the relative concentration of which depended on the catalyst temperature and the metal dispersion. At higher reaction temperatures, some of the multicarbonyl species were annihilated while the linear or the bridge-bonded CO adstates held at the large Ru clusters grew in number. In the multicarbonyl form, the inclined mode of adsorbed CO is likely to dissociate at a lower temperature compared to CO held in the linear or bridged mode at Ru_x sites.

3. The microcalorimetry data also point to a difference in the modes and stoichiometry of CO/H_2 adsorption, when the ruthenium metal and a Ru/TiO_2 catalyst were exposed

to $CO + H_2$. Thus, in the case of exposure of Ru metal to a $CO + H_2$ (1:4) pulse, the observed q_d ~50 kJ mol^{-1} corresponded to 1:1 adsorption of CO and H_2 molecules at distinct metal sites for all the reaction temperatures (Table 1). In the presence of excess H_2, a high q_d value of ~180–190 kJ mol^{-1} was observed at the temperatures above 425 K which suggested the simultaneous occurrence of $C_s + 4H_{(ad)} \rightarrow CH_{4(ad)}$ step. Contrary to this, the q_d values observed for Ru/TiO_2 catalyst indicated the formation of carbonyl species and these species reacted in the presence of coadsorbed H_2 to give CH_4 and high q_d values even at low temperatures (Fig. 11).

4. The reaction route followed in the CO methanation on a particular metal surface appears to depend on various factors such as the metal dispersion, nature of support, mode/stability of the CO adstates, and the concentration and mode of hydrogen adstates. No universal reaction mechanism must be envisaged for a particular metal. In the case of Ru/TiO_2, the formation and the transformations of

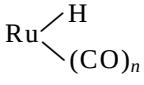

species at well-dispersed metal sites may control the kinetics of the CO methanation at low reaction temperatures (ca. <450 K). No such reaction route is plausible on bulk Ru surface, which showed no low temperature catalytic activity. At higher reaction temperatures, the catalytic activity arises due to dissociation of CO molecules, bonded in the linear or in the bridged forms over the bulk Ru metal or over the large Ru crystallites existing at Ru/TiO_2 surface. FTIR spectroscopy has provided evidence for the transformation of small metal particles to large Ru clusters at the high reaction temperatures, as is reported in the recent literature (9, 25).

ACKNOWLEDGMENT

We thank referees for critical comments and suggestions.

REFERENCES

1. Londhe, V. P., and Gupta, N. M., *J. Catal.* **169**, 415 (1997).
2. Gupta, N. M., Kamble, V. S., Iyer, R. M., Thampi, K. R., and Gratzel, M., *J. Catal.* **137**, 473 (1992).
3. Gupta, N. M., Kamble, V. S., Kartha, V. B., Thampi, K. R., and Gratzel, M., *J. Catal.* **146**, 173 (1994).
4. Kamble, V. S., Londhe, V. P., Gupta, N. M., Thampi, K. R., and Gratzel, M., *J. Catal.* **158**, 427 (1996).
5. Londhe, V. P., Kamble, V. S., and Gupta, N. M., *J. Mol. Catal.*, in press.
6. Vannice, M. A., and Garten, R. L., *J. Catal.* **63**, 255 (1980).
7. Miura, H. M., Mc Laughlin, M. L., and Gonzalez, R. D., *J. Catal.* **79**, 227 (1983).
8. Wedler, G., Papp, H., and Schroll, G., *J. Catal.* **38**, 153 (1975).
9. Solymosi, F., and Rasko, J., *J. Catal.* **115**, 107 (1989).
10. Yokomizo, G. H., Louis, C., and Bell, A. T., *J. Catal.* **120**, 1 (1989).
11. King, D. L., *ACS Preprints, Div. Petr. Chem.* **23**, 482 (1978).
12. Kiskinova, M., *in* "New Trends in CO Activation" (L. Guczi, Ed.), p. 37. Elsevier, Amsterdam, 1991.
13. Vannice, M. A., *in* "Catalysis: Science and Technology" (J. R. Anderson and M. Boudart, Eds.), Vol. 3, p. 139. Springer-Verlag, Berlin, 1982.
14. Joyner, R. W., *Surf. Sci.* **63**, 291 (1977).
15. Bradshaw, A. M., *Surf. Sci.* **80**, 215 (1979).
16. Pfnur, H., Menzel, D., Hoffmann, F. M., Ortega, A., and Bradshaw, A. M., *Surf. Sci.* **93**, 431 (1980).
17. Williams, E. D., and Weinberg, W. H., *Surf. Sci.* **82**, 93 (1979).
18. Yates, D. J. C., Murrell, L. L., and Prestridge, E. B., *J. Catal.* **57**, 41 (1979).
19. Yao, H. C., Japar, S., and Shelef, M., *J. Catal.* **50**, 407 (1977).
20. Bartholomew, C. H., and Pannell, R. B., *J. Catal.* **65**, 390 (1980).
21. Guerrero-Ruiz, A., *Appl. Catal.* **55**, 21 (1989).
22. Benndorf, C., Kruger, B., and Thieme, F., *Surf. Sci.* **163**, L675 (1985).
23. Shinn, N. D., and Madey, T. E., *Phys. Rev. Lett.* **53**, 2481 (1984).
24. Shinn, N. D., and Madey, T. E., *J. Chem. Phys.* **83**, 5928 (1985).
25. Mizushima, T., Tohji, K., Udagawa, Y., and Ueno, A., *J. Phys. Chem.* **94**, 4980 (1990).